Journal of Nuclear Medicine, published on February 3, 2022 as doi:10.2967/jnumed.121.263561

^{18}F-FDG Fetal Dosimetry Calculated with PET/MRI

Paolo Zanotti-Fregonara[1], Tatsuya Ishiguro[2], Kosuke Yoshihara[2], Shiro Ishii[3], Takayuki Enomoto[2]

[1]Molecular Imaging Branch, National Institute of Mental Health, Bethesda, Maryland

[2]Department of Obstetrics and Gynecology, Niigata University Medical & Dental Hospital, Niigata, Japan

[3]Department of Radiology and Nuclear Medicine, Fukushima Medical University Hospital, Fukushima, Japan

Submitted to *Journal of Nuclear Medicine* as an Original Article, November 2021

Correspondence

Dr. Paolo Zanotti-Fregonara

Molecular Imaging Branch, National Institute of Mental Health

10 Center Drive, MSC-1026, Bldg. 10, Rm. B1D43

Bethesda, MD 20892-1026

Phone: +1 301.451.8898

Email: zanottifregonp@nih.gov

Financial Disclosure

This work was supported in part by the Intramural Research Program of the National Institute of Mental Health, National Institutes of Health (project number ZIAMH002852).

Word Count: 4140

Running Title: ^{18}F-FDG fetal dosimetry and PET/MRI

ABSTRACT

The fetal absorbed dose from ^{18}F-FDG administration to the mother is an essential piece of information when considering the use of PET to stage cancers during pregnancy. However, the few existing human case reports were obtained using either PET-only or PET/CT machines, which may not accurately identify the soft tissues of the fetus for dosimetric calculations. This study presents data from 11 women injected with ^{18}F-FDG for cancer staging during the first two trimesters of pregnancy and is the first to be entirely acquired with PET/MRI.

Methods: Eleven pregnant women (12 scans) with cervical cancer were imaged with ^{18}F-FDG PET/MRI, and their images were retrospectively analyzed for this study. The fraction of injected activity concentrated by the fetus was derived from manually drawing regions of interest on the MRI slices. From the activity fraction, the fetal time-integrated coefficients were derived and combined with the standard coefficients of the mothers' organs from the ICRP publication 106. The fetal absorbed doses were calculated with OLINDA/EXM 1.1 and a dynamic bladder model.

Results: All fetuses after early pregnancy could be accurately delineated due to the coregistered MRI scans. ^{18}F-FDG activity was unevenly distributed in the fetal body: the hearts and the urinary bladders were generally visible, while the brain showed lower uptake. The estimated fetal doses were 2.21E-02 mGy/MBq for one woman imaged in early pregnancy, 7.38 ± 0.25 E-03 mGy/MBq for three women imaged at the end of the first trimester, and 4.92 ± 1.53 E-03 mGy/MBq for eight women imaged during the second trimester.

Conclusion: PET/MRI images of pregnant women injected with ^{18}F-FDG confirm that the fetal ^{18}F-FDG dose is very low. Therefore, clinically appropriate ^{18}F-FDG scans in women with cancer should not be withheld because of pregnancy.

Keywords: ^{18}F-FDG, pregnancy, fetal dosimetry, PET/MRI

INTRODUCTION

Given the critical role of ^{18}F-fluoro-2-deoxyglucose (^{18}F-FDG) in staging most types of cancer and the worldwide diffusion of positron emission tomography (PET) machines, the number of pregnant women injected with ^{18}F-FDG—either by mistake or by clinical necessity—is bound to increase. In this context, the dose to the fetus is essential to reach an informed clinical decision. Until relatively recently, fetal biokinetic data for ^{18}F-FDG were unknown. When Russell and colleagues compiled the first extensive database of fetal doses from different radiopharmaceuticals in 1997, no biological data were available; thus, the ^{18}F-FDG dose was calculated by considering only irradiation from maternal organs (*1*). Stabin revised these doses in 2004 on the basis of newly acquired monkey data (*2*), but the first case report of ^{18}F-FDG use in a pregnant woman was only published in 2008 (*3*). Since then, at least 20 different case reports have become available (*4*), and new dosimetric estimates based on human data have been proposed (*5*).

Although these advances allow a clearer picture of ^{18}F-FDG fetal uptake and dosimetry at different stages of pregnancy, more cases are needed to refine these values and to fill gaps during those periods of pregnancy where case data are not yet available. In addition, almost all previous dose estimates were derived from PET-only or positron emission tomography/computed tomography (PET/CT) images, where the soft tissues can sometimes be difficult to delineate. This study presents data from 11 pregnant women (12 scans) who were injected with ^{18}F-FDG for cancer staging during the first two trimesters of pregnancy and imaged with positron emission tomography/magnetic resonance imaging (PET/MRI).

MATERIALS AND METHODS

Patients

Eleven pregnant women with cervical cancer were imaged with ^{18}F-FDG PET/MRI, and their images were retrospectively analyzed for this study. The gestational age ranged from 9 to 24 weeks and was determined by measuring the crown-rump length by ultrasound examination at 9-10 gestational weeks, calculated from the last menstrual period. One woman was imaged twice at 18 and 24 weeks. Data for seven of these 11 women were previously published in a study that sought to assess the clinical utility of ^{18}F-FDG PET in cervical cancer (*6*). The patients were treated at the Niigata University Medical and Dental Hospital, Niigata, Japan, and the imaging was performed at the Fukushima Medical University Hospital using a Biograph mMR PET/MRI device equipped with a 3-T MRI (Siemens Healthcare). Acquisition details can be found in (*6*). The women were injected with approximately 4 MBq/kg of ^{18}F-FDG (average injected activity was 213 ± 52 MBq). The institutional ethics board of the National Institute of Mental Health approved this retrospective study and the requirement to obtain informed consent was waived.

Dosimetry calculations

The dosimetric calculations in this study closely followed the methodology proposed in (*4*), according to which pregnancy was divided into periods: early pregnancy (0-10 wks) where, given the small size of the fetus, the fetal dose was approximated to that of the uterus of a nonpregnant woman; the rest of the first trimester (11-13 wks); and the second trimester (14–26 wks). For these last two periods the digital phantoms representing pregnant women at the first and second trimester were used (*7*). None of the women was in the third trimester.

The fraction of injected activity concentrated by the fetus (or by the uterus for the only participant who was imaged during early pregnancy) was derived from manually drawing regions of interest on all MRI slices in which the fetus was visible (or around the whole uterus). All fetal regions of interest were drawn by an experienced imaging specialist (PZF), who also analyzed most of the cases

reported in the literature. The results of this study are therefore directly comparable to those previously published. From the activity fraction, the time-integrated coefficients were derived by considering the physical half-life of ^{18}F (1.83 hours) as the effective half-life of ^{18}F-FDG. The time-integrated activities were combined with those of the mothers' organs reported in publication 106 of the International Commission on Radiological Protection (ICRP) (*8*) (Table 1). Maternal bladder voiding was simulated with the following parameters: first fraction of 0.075 with a half-life of 0.2 hours, and second fraction of 0.225 with a half-life of 1.5 hours. The bladder-voiding interval was set at 1 hour. The absorbed doses were calculated by entering the time-integrated coefficients of both the mothers and the fetuses into OLINDA/EXM 1.1 (*9*).

The dose calculated with individual image-derived time-integrated coefficients was also compared with those extrapolated with the mathematical function proposed in (*10*). This function was obtained by fitting a sigmoid curve through the time-integrated coefficients of the cases available at the time of publication (*4*).

RESULTS

All fetuses were visible in detail on the MRI scans, which allowed the delineation of their body contours (Figure 1). ^{18}F-FDG activity was unevenly distributed in the fetal body. The hearts were generally visible, while the brain showed low uptake (Figures 2 and 3). The estimated fetal doses were 2.21E-02 mGy/MBq for the woman imaged during early pregnancy, 7.38 ± 0.25 E-03 mGy/MBq for the three women imaged at the end of the first trimester, and 4.92 ± 1.53 E-03 mGy/MBq for the eight women imaged during the second trimester (Table 2).

The doses extrapolated with the sigmoid function predicted the measured doses in the first 15 weeks of pregnancy well (within 10%). Starting from the 15th week, however, the extrapolated time-

integrated coefficients were lower than the measured coefficients (Figure 4); the measured doses were thus underestimated by up to 25% (Table 3).

DISCUSSION

This study, which contains the largest population ever published of pregnant patients imaged with ^{18}F-FDG, significantly expands the pool of available human dosimetric data. The available cases now cover the duration of pregnancy until the 34th week, with an approximate frequency of at least one case every two weeks (Table 2). Notably, previously available case reports left a gap between the 12th and the 18th weeks. Because the present study includes eight scans acquired between the 13th and the 18th weeks, a more complete picture of ^{18}F-FDG uptake during pregnancy is now available. It is also important to note that, after the 34th week, dosimetry is not likely to change significantly because ^{18}F-FDG uptake by the fetus tends to plateau (Figure 4). In addition, late-pregnancy dosimetry might be clinically less valuable, because scans can more easily be postponed until delivery or labor can be induced, since the fetus is already viable.

Importantly, all women in this study were scanned with PET/MRI, which allowed a detailed delineation of the fetal body contours and hence dose estimations were arguably more accurate. Such accuracy cannot be achieved by coregistering the PET to an MRI acquired separately because the fetus would have moved in the meantime. In the present study, fetal movements were likely to be minimal because excellent coregistration of MRI and PET was observed in all cases; an example of this is visible in the superposition of the fetal heart on MRI and myocardial ^{18}F-FDG activity in Figures 2 and 3. In addition to providing an excellent visualization of the fetal body, PET/MRI machines do not deliver to the fetus the additional dose of a CT scan or of a transmission source and therefore, if available, should preferentially be used to image pregnant women.

The MRI images allowed drawing the fetal regions of interest with a high level of confidence, so that inaccuracies due to manual segmentation could be minimized. Of course, since there is no "gold standard" against which the segmentations can be compared, residual segmentation errors cannot be quantified. However, it is reasonable to assume that fetal regions of interest drawn on an MRI are more accurate than those drawn directly from PET, where fetal contours are not visible (Figure 1), or CT, where fetal soft tissues are difficult to delineate. The present dose estimates confirmed the low level of radiation absorbed by the fetus when the mother is injected with ^{18}F-FDG. The highest estimate was observed in early pregnancy (3.2 mGy), but the average of the remaining cases was 1.1 ± 0.5 mGy. The fetus of the woman who had two examinations received a cumulative dose of 3.3 mGy. These values would not significantly change if different anthropomorphic phantoms were used (*4,11,12*) and are more than one order of magnitude lower than the threshold for deterministic effects. While stochastic effects cannot technically be ruled out, no effects have ever been observed for doses this low (*13*). Taken together, these data suggest that the benefits for both mother and fetus of a clinically appropriate ^{18}F-FDG PET scan outweigh the hypothetical risks to the fetus theorized by the linear no-threshold model (*14,15*). Notably, in the case of cervical cancers, the primary tumor size may be evaluated with MRI, but to assess lymph-node involvement the alternative to PET/MRI may be an invasive histological verification.

To compensate for the incomplete data coming from sparse published case reports, we previously used mathematical modeling to extrapolate the time-integrated coefficients for the whole duration of pregnancy from available human cases (*10*). We found that the variation of the fetal time-integrated coefficients follows a sigmoid function: after a rapid increase in the second trimester and the beginning of the third, when the fetal mass rapidly increases, the function eventually tends to plateau when the fetus reaches maturity (Figure 4). Building on that work, the present study prospectively tested whether the doses extrapolated by the function could predict the calculated doses. Our findings

demonstrated that the extrapolated doses closely match the calculated doses until the 15th week of pregnancy but underestimate the doses by up to 25% between the 14th and 25th weeks (Table 3). An error of up to 25% could be considered minor compared with the uncertainties in internal dose estimations (*16,17*) and, indeed, larger differences are observed between the measured values in different fetuses at the same week of pregnancy (Table 2). On the other hand, the actual dose was underestimated in eight of 11 fetuses, including all the fetuses starting at the 14th week (Table 3), which suggests the possibility of a systematic group difference. One possible source of this difference is ethnicity; specifically, this study comprised Japanese women (average weight 59 ± 12 kg), while the populations used to build the mathematical function comprised American and European women (average weight 73 ± 13 kg). Another possible reason for a systematic group difference is that previously published cases were acquired mostly with PET, where fetal contours were not visible, or PET/CT, where fetal soft tissues were sometimes difficult to delineate or to differentiate from placental uptake (*18*); in contrast, all the fetuses in this study were visible in detail thanks to the simultaneous MRI. For example, when creating the original sigmoid curve, one datapoint was automatically eliminated as an outlier during the fitting process (Figure 4). Because this point was from a PET only study, it is possible that the segmentation of that fetal body was inaccurate.

Finally, it should be noted that the cases in the present paper, as well as all the other cases published in the literature to date, consist of static images. In consequence, some (conservative) assumptions must be made to calculate the dose, such as considering the physical half-life of ^{18}F equal to the effective half-life of ^{18}F-FDG. It is likely that the fetal dose calculated with measured time-integrated coefficients will be slightly lower. If the PET scan of a pregnant woman is planned, we encourage nuclear medicine departments to acquire dynamic images. These would not increase the radiation dose but would allow an even more accurate assessment of fetal dosimetry as well as enable, for the first time, calculation in vivo of the metabolic rate of glucose in the various fetal tissues with full

kinetic modeling. Given the absence of radiometabolites, ^{18}F-FDG activity in the mother's aorta would provide an excellent image-derived input function. Recent scanners—which allow fast dynamic images of excellent quality to be obtained over the whole body even with lower injected activities (*19*)—may yield input functions of such quality that they could reliably be used in conjunction with the gold standard of compartmental modeling rather than only with graphical analyses (*20*). This would enable a deeper understanding of the physiology of glucose utilization in the fetus and its evolution over the duration of pregnancy.

CONCLUSION

PET/MRI images of pregnant women injected with ^{18}F-FDG confirm that the fetal ^{18}F-FDG dose is very low. Therefore, clinically appropriate ^{18}F-FDG scans in women with cancer should not be withheld because of pregnancy.

FINANCIAL DISCLOSURE

This work was supported in part by the Intramural Research Program of the National Institute of Mental Health, National Institutes of Health (project number ZIAMH002852).

DISCLAIMER

The authors have no conflict of interest to disclose, financial or otherwise. The views expressed in this commentary do not necessarily represent the views of the National Institutes of Health, the Department of Health and Human Services, or the United States Government.

ACKNOWLEDGEMENTS

The authors thank Ioline Henter (NIMH) for invaluable editorial assistance.

KEY POINTS

QUESTION: What is the ^{18}F-FDG fetal dosimetry in pregnant women with cancer imaged with PET/MRI?

PERTINENT FINDINGS: Dosimetric values estimated with PET/MRI confirm that the ^{18}F-FDG fetal dose is very low.

IMPLICATIONS FOR PATIENT CARE: Clinically appropriate ^{18}F-FDG scans in women with cancer should not be withheld because of pregnancy.

REFERENCES

1. Russell JR, Stabin MG, Sparks RB. Placental transfer of radiopharmaceuticals and dosimetry in pregnancy. *Health Phys.* 1997;73:747-755.

2. Stabin MG. Proposed addendum to previously published fetal dose estimate tables for 18F-FDG. *J Nucl Med.* 2004;45:634-635.

3. Zanotti-Fregonara P, Champion C, Trebossen R, Maroy R, Devaux JY, Hindie E. Estimation of the beta+ dose to the embryo resulting from 18F-FDG administration during early pregnancy. *J Nucl Med.* 2008;49:679-682.

4. Zanotti-Fregonara P, Chastan M, Edet-Sanson A, et al. New Fetal Dose Estimates from 18F-FDG Administered During Pregnancy: Standardization of Dose Calculations and Estimations with Voxel-Based Anthropomorphic Phantoms. *J Nucl Med.* 2016;57:1760-1763.

5. Stabin MG. New-Generation Fetal Dose Estimates for Radiopharmaceuticals. *J Nucl Med.* 2018;59:1005-1006.

6. Ishiguro T, Nishikawa N, Ishii S, et al. PET/MR imaging for the evaluation of cervical cancer during pregnancy. *BMC Pregnancy Childbirth.* 2021;21:288.

7. Stabin M, Watson E, Cristy M, et al. Mathematical Models and Specific Absorbed Fractions of Photon Energy in the Nonpregnant Adult Female and at the End of Each Trimester of Pregnancy. *ORNL Report ORNL/TM-12907.* 1995.

8. International Commission on Radiological Protection (ICRP). ICRP Publication 106: Radiation Dose to Patients from Radiopharmaceuticals - Addendum 3 to ICRP Publication 53. *Ann ICRP.* 2008;38 (1-2).

9. Stabin MG, Sparks RB, Crowe E. OLINDA/EXM: the second-generation personal computer software for internal dose assessment in nuclear medicine. *J Nucl Med.* 2005;46:1023-1027.

10. Zanotti-Fregonara P, Stabin MG. New Fetal Radiation Doses for (18)F-FDG Based on Human Data. *J Nucl Med.* 2017;58:1865-1866.

11. Stabin M, Farmer A. OLINDA/EXM 2.0: The new generation dosimetry modeling code. *Journal of Nuclear Medicine.* 2012;53:585-585.

12. Zanotti Fregonara P. Radiation absorbed dose to the embryo and fetus from radiopharmaceuticals. *Semin Nucl Med.* 2022;In press.

13. Brent RL. Saving lives and changing family histories: appropriate counseling of pregnant women and men and women of reproductive age, concerning the risk of diagnostic radiation exposures during and before pregnancy. *Am J Obstet Gynecol.* 2009;200:4-24.

14. Zanotti-Fregonara P, Hindie E. Performing nuclear medicine examinations in pregnant women. *Phys Med.* 2017;43:159-164.

15. Zanotti-Fregonara P. Pregnancy should not rule out (18)FDG PET/CT for women with cancer. *Lancet.* 2012;379:1948-1948.

16. Stabin MG. Uncertainties in internal dose calculations for radiopharmaceuticals. *J Nucl Med.* 2008;49:853-860.

17. Gear JI, Cox MG, Gustafsson J, et al. EANM practical guidance on uncertainty analysis for molecular radiotherapy absorbed dose calculations. *Eur J Nucl Med Mol Imaging.* 2018;45:2456-2474.

18. Zanotti-Fregonara P, Jan S, Champion C, et al. In vivo quantification of 18f-fdg uptake in human placenta during early pregnancy. *Health Phys.* 2009;97:82-85.

19. Vandenberghe S, Moskal P, Karp JS. State of the art in total body PET. *EJNMMI Physics.* 2020;7:35.

20. Zanotti-Fregonara P, Chen K, Liow JS, Fujita M, Innis RB. Image-derived input function for brain PET studies: many challenges and few opportunities. *J Cereb Blood Flow Metab.* 2011;31:1986-1998.

21. Zanotti-Fregonara P, Laforest R, Wallis JW. Fetal Radiation Dose from 18F-FDG in Pregnant Patients Imaged with PET, PET/CT, and PET/MR. *J Nucl Med.* 2015;56:1218-1222.

22. Takalkar AM, Khandelwal A, Lokitz S, Lilien DL, Stabin MG. 18F-FDG PET in pregnancy and fetal radiation dose estimates. *J Nucl Med.* 2011;52:1035-1040.

23. Zanotti-Fregonara P, Jan S, Taieb D, et al. Absorbed 18F-FDG dose to the fetus during early pregnancy. *J Nucl Med.* 2010;51:803-805.

24. Zanotti-Fregonara P, Koroscil TM, Mantil J, Satter M. Radiation dose to the fetus from [18F]-FDG administration during the second trimester of pregnancy. *Health physics.* 2012;102:217.

25. Calais J, Hapdey S, Tilly H, Vera P, Chastan M. Hodgkin's Disease Staging by FDG PET/CT in a Pregnant Woman. *Nucl Med Mol Imaging.* 2014;48:244-246.

26. Erdogan EB, Ekmekcioglu O, Vatankulu B, Ergul N, Demir M, Sonmezoglu K. An unknown pregnancy at term detected by a FDG-PET/CT study in a patient with Hodgkin's lymphoma: A case report. *Rev Esp Med Nucl Imagen Mol.* 2015;34:201-202.

FIGURE LEGENDS

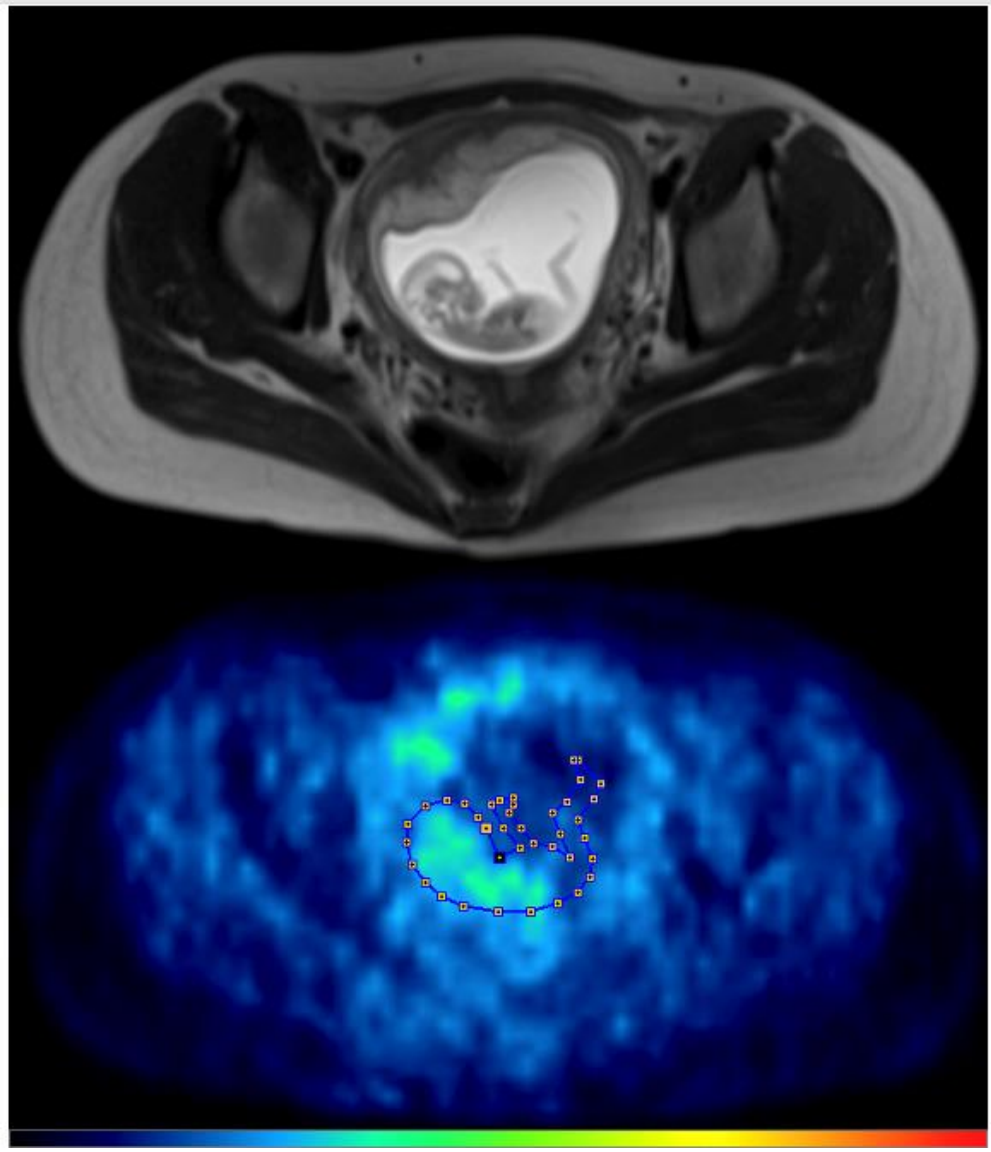

Figure 1. Transaxial images of MRI and PET in a woman at 13 weeks of pregnancy. The fetus is visible in minute detail on the MRI, including body parts, such as limbs, that are “cold” on the PET images. The figure demonstrates how the region of interest drawn around the fetal body, shown superimposed to the PET scan below, would not have been drawn with this shape if only PET images had been available. It is thus reasonable to hypothesize that fetal dosimetry obtained with PET/MRI is more accurate than that obtained with PET-only or PET/CT scans.

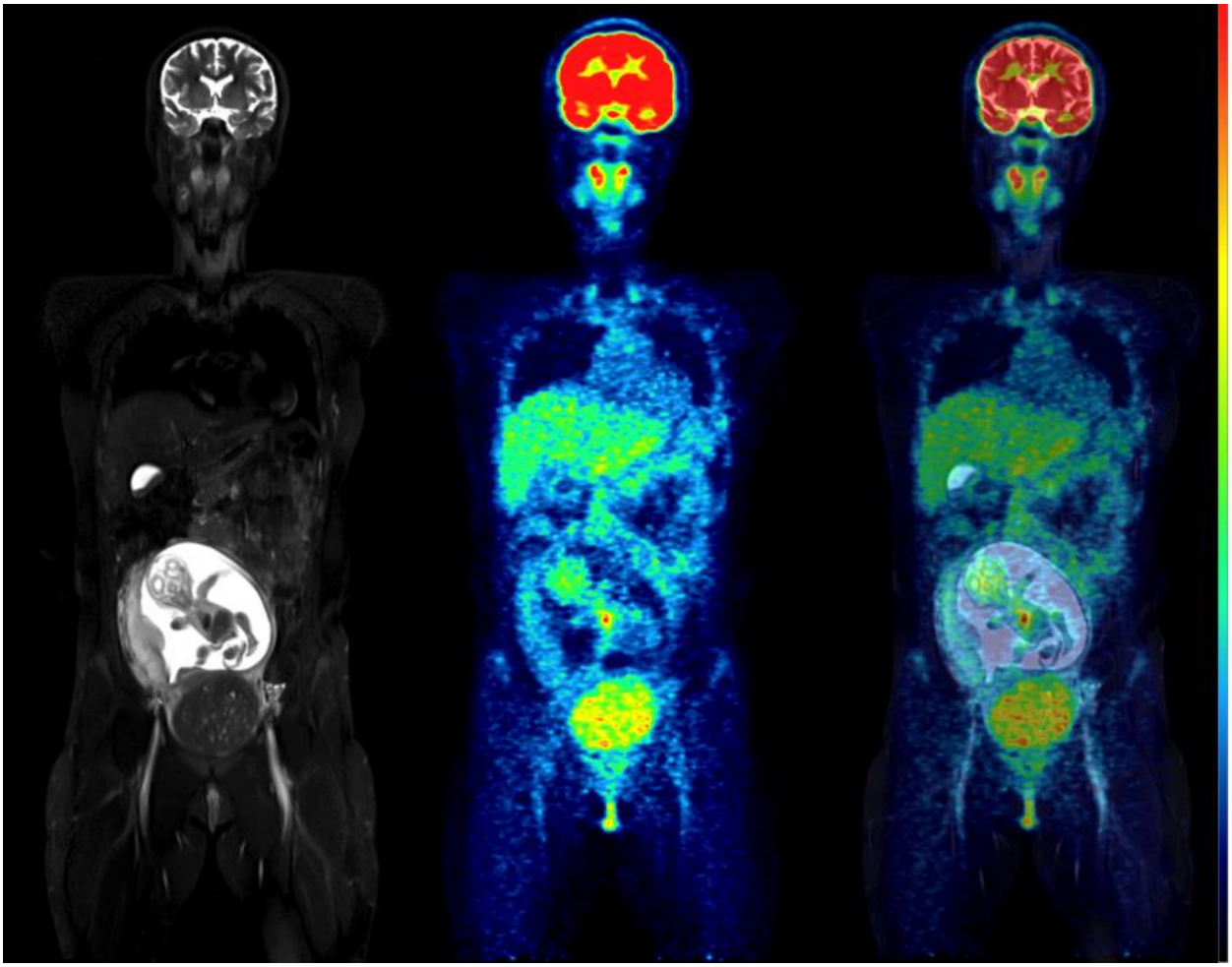

Figure 2. Coronal slices of MRI (left), PET (center), and fused PET/MRI (right) of a woman in the 18th week of pregnancy. Of particular interest is the level of uptake in the fetal organs. While the heart showed high ^{18}F-FDG uptake, the brain had only a low level of glucose consumption, especially compared with the brain uptake of the mother. This pattern of low glucose consumption has previously been noted even in mature fetuses (*4*).

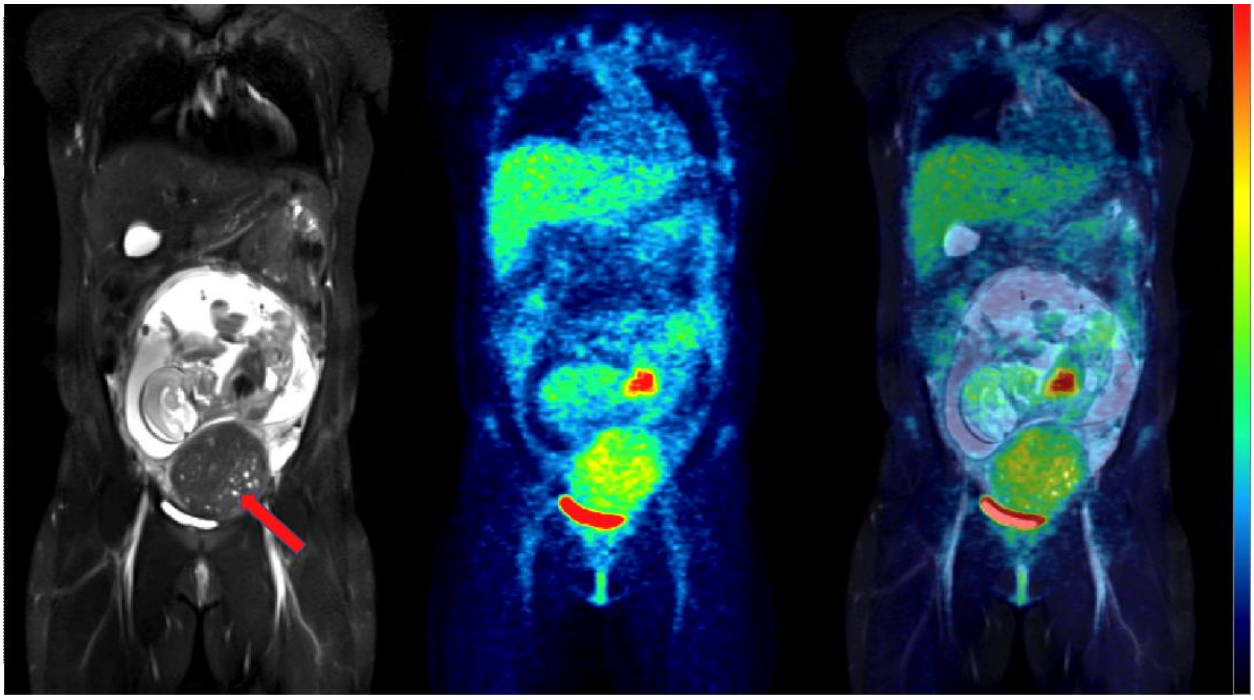

Figure 3. Coronal slices of MRI (left), PET (center), and fused PET/MRI (right) of the same woman in Figure 2, but at 24 weeks of pregnancy. The fetus has visibly increased in mass, but the pattern of ^{18}F-FDG uptake in the organs has not changed, with the heart showing high glucose consumption but the brain still largely silent. The red arrow points to a uterine fibroid.

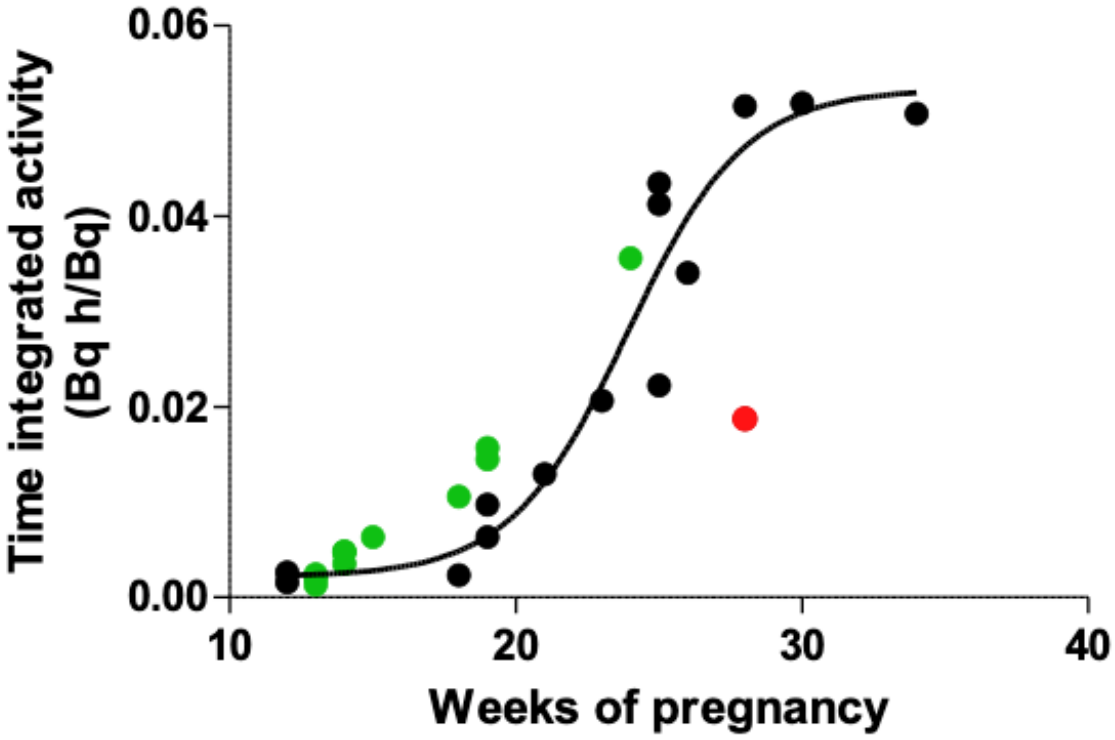

Figure 4. Sigmoid function fitted through the measured time-integrated activity data points (black dots), as reported in (*10*). During the fitting of the original curve, the automatic detection of outliers (ROUT [robust regression and outlier removal] Q coefficient, 1.0%) removed one point (in red). This outlying red point came from a PET-only study, which raises the possibility of inaccurate segmentation of the fetal body on the PET images. The datapoints of the patients of the present study (in green) tended to be higher than the extrapolated values. Although the difference was modest, this points to the possibility of a systematic group difference (see text for discussion).

Table 1 Time-Integrated Activities for Mothers' Organs, Taken from ICRP 106 (*8*)

Organ	Time-integrated activity (Bq h/Bq)
Brain	0.21
Heart wall	0.11
Lungs	0.079
Liver	0.13
Rest of the body	1.7

Fetus	Stage of gestation	Mother's weight (kg)	Injected Activity (MBq)	Machine	Phantom (trimester)	Fraction	Time-integrated activity (Bq h/Bq)	Dose (mGy/MBq)	Reference
1	5 wks	86	296	PET/CT	Nonpregnant	0.0012	0.0030	1.73E–02	(*21*)
2	6 wks	68	583	PET	Nonpregnant	0.0036	0.0095	3.14E–02	(*22*)
3	8 wks	60	320	PET/CT	Nonpregnant	0.0020	0.0053	2.23E–02	(*3*)
4	9 wks	50	144	PET/MRI	Nonpregnant	0.0019	0.0052	2.21E-02	This study
5	10 wks	71	296	PET/CT	Nonpregnant	0.0018	0.0046	2.08E–02	(*23*)
6	12 wks	58	385	PET/CT	1	0.0006	0.0016	7.25E–03	(*21*)
7	~12 wks	77	350	PET	1	0.0010	0.0026	7.70E–03	(*21*)
8	13 wks	64	178	PET/MRI	1	0.0005	0.0013	7.11E-03	This study
9	13 wks	53	209	PET/MRI	1	0.0007	0.0020	7.43E-03	This study
10	13 wks	52	205	PET/MRI	1	0.0009	0.0024	7.61E-03	This study
11	14 wks	86	333	PET/MRI	2	0.0013	0.0035	3.69E-03	This study
12	14 wks	48	187	PET/MRI	2	0.0018	0.0047	3.87E-03	This study
13	14 wks	49	199	PET/MRI	2	0.0018	0.0048	3.88E-03	This study
14	15 wks	59	235	PET/MRI	2	0.0028	0.0063	4.10E-03	This study
15	18 wks #	67	189	PET/MRI	2	0.0040	0.0106	4.72E-03	This study
16	18 wks ##	88	200	PET	2	0.0009	0.0023	3.52E–03	(*22*)
17	19 wks	51	348	PET/MRI	2	0.0024	0.0063	4.10E–03	(*21*)
18	19 wks	70	296	PET/MRI	2	0.0037	0.0097	4.59E–03	(*21*)
19	19 wks	50	197	PET/MRI	2	0.0059	0.0157	5.46E-03	This study
20	19 wks	48	187	PET/MRI	2	0.0055	0.0145	5.28E-03	This study
21	21 wks	53	181	PET/CT	2	0.0049	0.0129	5.05E–03	(*24*)
22	23 wks	59	181	PET	2	0.0078	0.0206	6.17E–03	(*22*)
23	24 wks #	70	291	PET/MRI	2	0.0135	0.0356	8.33E-03	This study
24	25 wks	67	337	PET	2	0.0084	0.0222	6.40E–03	(*22*)
25	25 wks $	76	188	PET/CT	2	0.0156	0.0412	9.14E–03	(*4*)
26	25 wks $	76	188	PET/CT	2	0.0164	0.0434	9.46E–03	(*4*)
27	26 wks	81	242	PET/CT	2	0.0129	0.0340	8.10E–03	(*25*)
28	28 wks	82	174	PET	3	0.0071	0.0187	3.38E–03	(*22*)
29	~28 wks	66	296	PET	3	0.0195	0.0515	6.22E–03	(*21*)
30	30 wks ##	89	229	PET	3	0.0196	0.0518	6.24E–03	(*22*)
31	34 wks	95	555	PET/CT	3	0.0192	0.0507	6.15E–03	(*26*)

and ##: Women imaged twice during pregnancy; $ Twin pregnancy

Table 2: Dosimetry results for the fetuses in the present study (in red) compared to cases previously reported in the literature (in black). The references show the publication where the cases were originally described. The doses may differ from those reported in the original publication, when they were reanalyzed in a standardized way (*4*).

Table 3: Comparison between the doses extrapolated from the mathematical function described in (*10*) and the doses measured in this study, starting after early pregnancy.

Stage of gestation	Phantom (trimester)	Measured time-integrated activity (Bq h/Bq)	Extrapolated time-integrated activity (Bq h/Bq)	Measured Dose (mGy/MBq)	Extrapolated Dose (mGy/MBq)	% Difference between the measured and extrapolated doses
13 wks	1	0.0013	0.00241	7.11E-03	7.61E-03	7.0
13 wks	1	0.0020	0.00241	7.43E-03	7.61E-03	2.4
13 wks	1	0.0024	0.00241	7.61E-03	7.61E-03	0.0
14 wks	2	0.0035	0.00256	3.69E-03	3.56E-03	-3.5
14 wks	2	0.0047	0.00256	3.87E-03	3.56E-03	-8.0
14 wks	2	0.0048	0.00256	3.88E-03	3.56E-03	-8.2
15 wks	2	0.0063	0.00281	4.10E-03	3.59E-03	-12.4
18 wks #	2	0.0106	0.00485	4.72E-03	3.89E-03	-17.6
19 wks	2	0.0157	0.00641	5.46E-03	4.11E-03	-24.7
19 wks	2	0.0145	0.00641	5.28E-03	4.11E-03	-22.2
24 wks #	2	0.0356	0.02836	8.33E-03	7.29E-03	-12.5

Woman imaged twice during pregnancy

Graphical abstract